Non-linear Finite Element Analysis of Cracked A–517 Steel Compact Tension Specimens

R. B. BHAGAT, M. F. AMATEAU and M. L. CROCKEN
Applied Research Laboratory, The Pennsylvania State University, P.O. Box 30, State College, PA 16804, USA

ABSTRACT

This manuscript describes the two-dimensional non-linear finite element analysis on compact tension specimens of A-517 structural steel. The numerical analysis enables us to study the behavior of crack in a typical ductile material under external loading. Local (or nodal) strain energy density at all nodes inside and outside the crack tip plastic zone at several external loads is numerically computed. In the expected crack propagation direction, i.e., 0 degree in compact tension specimens, the local strain energy density first decreases with increasing distance from crack tip but then at a critical distance it increases. This distinct behavior of the local strain energy density ahead of a crack is load dependent. The details of the numerical analysis are presented for a series of compact tension specimens having a wide range of crack length-to-width ratio (0.25 to 0.88). Based on our numerical results, we have proposed three parameters: (a) a critical load for the initiation of crack growth, (b) a crack length dependent local strain energy parameter associated with the initiation of crack growth, and (c) a material characteristic local strain energy parameter associated with the brittle fracture or plastic collapse of the ductile material.

KEYWORDS

Non-linear finite element analysis; compact tension specimen; A-517 steel; crack growth; ductile material; strain energy density; crack tip plastic zone; crack propagation direction; brittle fracture; plastic collapse.

INTRODUCTION

Cracked ductile structures, at times, pose formidable problems in reliably predicting the crack growth and subsequent failure of the structures. Generally, it is accepted that it is difficult, if not impossible, to obtain exact solutions in ductile structures encountering large scale yielding. Recent developments in finite element method (Bathe, 1982; Cook, 1981; Owen and Hinton, 1980; Zienkiewicz, 1983) have led to the numerical analysis of cracked ductile structures by several investigators (de Koning, 1977; Hilton and Sih, 1973; Lee and Liebowitz, 1977; Sih, 1974, 1977; Sih and

Hartranft, 1980; Sih and Madenci, 1983; Twickler et al., 1983). The finite element method and modern computers have provided advanced tools to carry out precise stress analysis even in the presence of large scale yielding. However, in order to develop a better understanding of the mechanical behavior of cracked ductile structures, there is still a need of further investigations for reliably predicting the initiation of crack growth followed by slow (steady) crack growth and fast (unsteady) crack growth leading to fracture of ductile structures.

The objectives of the present investigation are, therefore, twofold: (a) to carry out two-dimensional non-linear finite element analysis of high strength high stiffness ductile material with a wide range of crack length-to-width ratio and (b) to numerically predict the initiation of crack growth, slow crack growth and catastrophic fracture.

NUMERICAL ANALYSIS

Approach

A basic characteristic of all materials is their ability to absorb a certain amount of strain energy irrespective of how they are externally loaded (Gillemot, 1976). It is likely, therefore, that numerically computed local (nodal) strain energy density in a cracked ductile structure may reveal some unique behavior as a result of the crack tip plastic zone. This behavior may be different from the one in which the strain energy decays monotonically from the crack tip. With this premise, two-dimensional plane strain non-linear finite element analysis has been carried out to compute nodal strain energy density in cracked ductile material over a wide range of crack length-to-width ratios (0.25 to 0.88) at different external loads. The computer program used in the present investigation is a modified version of PAPST computer program (Hilton and Gifford, 1983) which uses two-dimensional 12-node isoparametric element and 4 × 4 numerical integration (Gaussian quadrature) to evaluate tangent stiffness matrices among other unique features. The modified program includes an iterative procedure under the restrictions of problem-dependent convergence criteria generated by the computer and the calculation of nodal strain energy density.

Procedure

A high strength high toughness structural steel (A-517) has been chosen for the finite element analysis. This steel exhibits a non-linear elastic-plastic response. A true stress-true strain diagram taken from published data (Hucek, 1981) is shown in Fig. 1. A multi-linear approach was used to model the curve of Fig. 1. Figure 2 shows a typical idealization of one of the several compact tension specimens used in the present investigation. As mentioned earlier, the finite element analysis has been carried out for several specimens having a wide range of crack length-to-width ratio (0.25 to 0.88).

The strain energy density for a node at (r,θ) from crack tip at a particular external load P is computed as follows: (i) the particular location (r,θ) is first checked by the computer program for yielding at different loads up to P. (ii) If the yielding occurs, the local (nodal) strain energy density is computed in the following three steps: (a) a series of values for numerically obtained effective loads (von Mises stresses) between zero and P are generated and stored; (b) a best-fit curve is plotted for effective stress and effective strain; and (c) the area under the curve, i.e., the local strain energy density, is numerically determined. (iii) If the

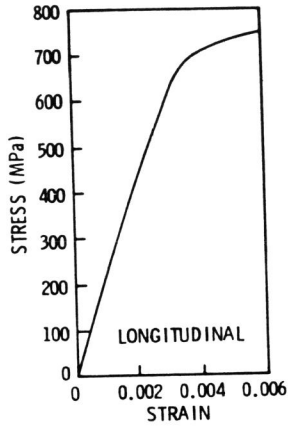

Fig. 1. True stress-true strain diagram for A-517 steel (Hucek, 1981).

yielding doesn't occur, Eq. (1) is used to calculate the local strain energy density.

$$\frac{dW}{dV} = \frac{1}{2E}\left[\sigma_x^2 + \sigma_y^2 + \sigma_z^2 - 2\nu(\sigma_x\sigma_y + \sigma_y\sigma_z + \sigma_x\sigma_z)\right] + \frac{\tau_{xy}^2}{2G} \qquad (1)$$

where σ_x, σ_y, σ_z are the normal stresses, τ_{xy} is the normal shearing stress, E is Young's modulus, G is the shear modulus, and ν is Poisson's ratio.

RESULTS AND DISCUSSION

Non-linear finite element analysis has been carried out for a large number of idealizations to cover a wide range of crack length-to-width ratio (0.25 to 0.88). Trial computations have been made for each idealization to optimize the scheme of load increments.

Local strain energy density (dW/dV) has been computed at each node in an idealization at various loads by the numerical analysis procedure described in the previous section. In Fig. 3, nodal (or local) strain energy density values at a particular load have been plotted against the radial distance of all nodes representing a wide range of angular positions (global analysis). It can be seen from Fig. 3 that not all values of energy density fall within an arbitrary marked monotonic band of the local strain energy density. This phenomenon was observed at several loads and for different crack lengths indicating that there exists a distinctly different behavior of local strain energy density for certain nodes ahead of a crack tip. In order to delineate the angular dependence of the nodal strain energy density, we plot the strain energy density at three selected angles (0 degree, 30 degrees and 50 degrees from crack tip) against the radial distance of the nodes in those angles (see Fig. 4).

We found that the energy values outside the band of Fig. 3 correspond to nodes in 0 degree direction from the crack tip. This direction is the

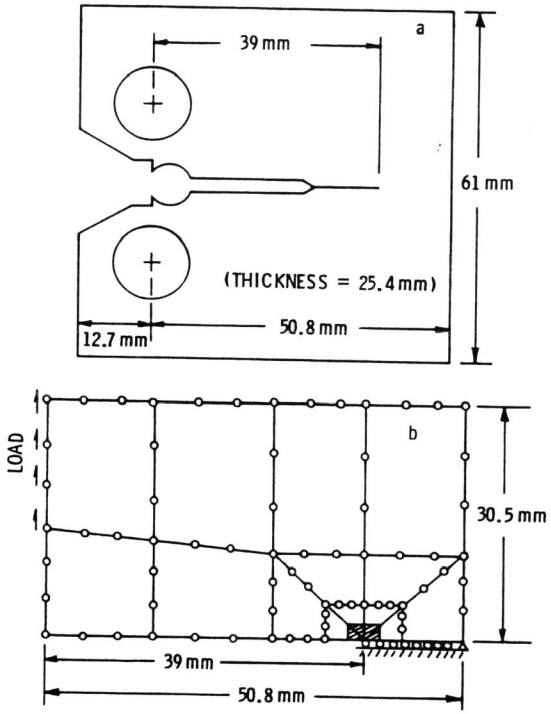

Fig. 2. Compact tension specimen geometry (a) and a typical finite element idealization (b). There are about 20 elements in the shaded area surrounding the crack tip (b).

expected direction of crack propagation in compact tension specimens. Next, we attempted to study the variation of the 0 degree nodal strain energy density against external loads and plotted several curves as seen in Fig. 5. The nodal energy density first decreases with increasing distance from the crack tip but then at a particular distance it increases. This distance is initially r_o at a relative low load and it decreases with increasing load until a critical load P_{cr}. For loads $\geq P_{cr}$, r_o reduces to a fixed value r_o^*. At the critical load (apparently between 21 kN and 24 kN in Fig. 5), the dW/dV vs r curve further shows that over a certain distance $r \geq 8.6$ mm (approximately) the nodal energy density almost remains constant (Fig. 5). For the sake of clarity, the dW/dV vs r curve at P_{cr} (22.15 kN as determined by plotting several dW/dV vs r curves as in Fig. 5 at loads greater than 21 kN) is drawn in Fig. 6 for extended range of dW/dV. The critical minimum energy value at r_o^* is designated $(dW/dV)^*_{min}$. At a distance r_p^* from the crack tip, dW/dV attains a value which remains constant for $r \geq r_p^*$ (up to or very close to the right face of the specimens, depending on the crack length); this critical energy value is designated as $(dW/dV)^*_p$ where the subscript p denotes the observed plateau in Fig. 6. No such energy plateau is observed at loads $> P_{cr}$. Figure 7 shows the load-dependence of minimum

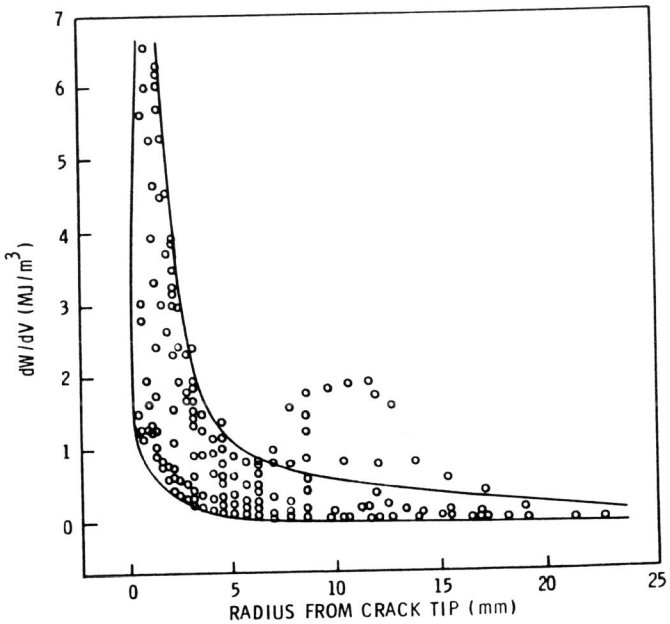

Fig. 3. Global analysis data for local strain energy density (dW/dV) for a crack length of 39.04 mm at a load of 21.35 kN. The plot shows the dependence of the nodal values of dW/dV on the radial distance of the nodes from the crack tip, irrespective of their angular positions.

strain energy density $(dW/dV)_{min}$ obtained from Fig. 5 and other similar plots. Up to a relatively lower load P_1 (Region I in Fig. 7) the minimum value of strain energy density designated as $(dW/dV)_{min}$ remains essentially constant beyond r_o (see Fig. 5, plot corresponding to 5.34 kN as an example). In Region II of Fig. 7, there is a distinct minimum for dW/dV at any load P between P_1 and P_{cr} (see Fig. 5). We propose that the necessary condition (i.e., the presence of a minimum value of the strain energy density at a fixed location ahead of the crack tip) for crack growth initiation has been met at this stage. However, the crack is still stable (i.e., slow crack growth has not initiated yet) because at higher loads within this region ($P_1 < P < P_{cr}$) the value of $(dW/dV)_{min}$ increases. This signifies that the cracked structure is simply gaining more energy because of the increased load. As soon as the load reaches P_{cr}, the material at $(r_o^*,0)$ has gained the maximum energy that it can absorb and $(dW/dV)_{min}$ reaches its maximum value (peak in Fig. 7) designated as $(dW/dV)^*_{min}$ (this should not be confused with maximum value of dW/dV). This condition of a critical load P_{cr} is considered sufficient (i.e., the minimum strain energy density at a fixed location $(r_o^*,0)$ attains its maximum value) for the initiation of crack growth. At any load higher than P_{cr}, $(dW/dV)_{min}$ decreases instead of increasing and thus the crack remains

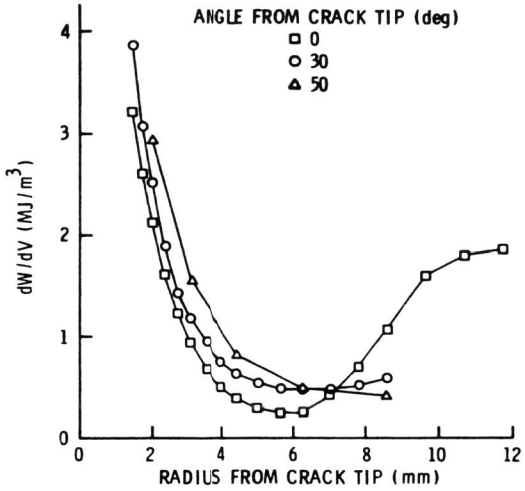

Fig. 4. Comparison of local strain energy density versus radial distance for nodes at three different angles from the crack tip at a load of 18.68 kN for a crack length of 39.04 mm.

susceptible for further growth. Moreover, the end of Region II is considered the end of "local instability" described here as a phenomenon satisfying the necessary as well as sufficient conditions for the initiation of crack growth.

The local instability is followed by stable slow crack growth (Region III) and fracture (Region IV), see Fig. 7. As explained above, at loads higher than P_{cr}, the crack remains vulnerable for further growth and stable crack growth occurs. The end of the stable crack growth (Region III) at a much higher load marks the small range of "global instability" described here as a phenomenon responsible for the unstable fracture of ductile materials. The load towards the end of Region III is almost equal to the extrapolated (dotted line in Fig. 7) fracture load P_f corresponding to a zero value of $(dW/dV)_{min}$. Thus, any possible significance of the end of the stable crack growth (Region III) is limited by the stability of finite element solutions at higher loads close to the fracture of the cracked structures as demonstrated by our finite element analysis.

Analysis of a wide range of crack length yields $(dW/dV)_{min}$ versus load plots similar in shape to the one shown in Fig. 7 and three such plots corresponding to three selected crack lengths are shown in Fig. 8. It can be seen from Fig. 8 that P_{cr} and P_f increase for reduced crack length. This is consistent with our expectation. Also, from Fig. 8 it is revealed that the ratio of P_{cr} to P_f remains constant with a value of 0.83, irrespective of the crack length. The theoretical significance of this constant ratio is not obvious. However, it is suggested that this ratio may be a characteristic of ductile materials. From an experimental value of P_f for any crack length, the value of P_{cr} can be immediately calculated assuming

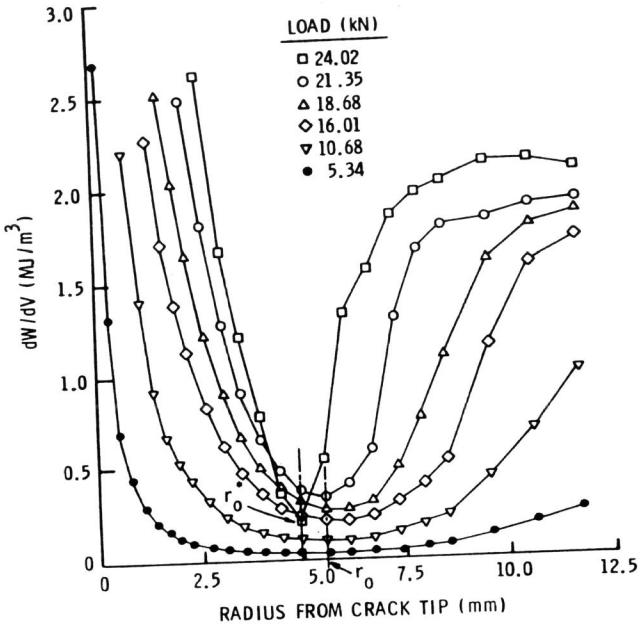

Fig. 5. Comparison of local strain energy density (for nodes at 0 degree from the crack tip) versus radial distance plots at several loads for a crack length of 39.04 mm.

that P_{cr}/P_f is equal to 0.83. Computer analysis will provide a dW/dV vs r curve similar to that in Fig. 6. This will lead to the establishment of $(dW/dV)^*_{min}$ and $(dW/dV)^*_p$ at a much reduced effort and computer time. Alternatively, for any crack length, the fracture load can be predicted by carrying out computer analysis up to loads slightly above P_{cr} in order to establish a peak for $(dW/dV)_{min}$ as in Fig. 7.

This investigation also reveals that $(dW/dV)^*_p$ is independent of crack length-to-width ratio and $(dW/dV)^*_{min}$ depends only to some extent on crack length-to-width ratio (Figs. 9 and 10). A brief explanation of potential significance of these energy parameters follows. With reference to Region II in Fig. 7, we stated that $(dW/dV)^*_{min}$ signifies the local instability responsible for the initiation of crack growth. The phenomenon of the local instability in ductile materials is most likely to depend on crack length and crack tip plastic zone. The higher the crack length, relatively lower the crack tip plastic zone before the necessary and sufficient conditions of the local instability are satisfied. This will in effect lead to a somewhat lower value of $(dW/dV)^*_{min}$ consistent with the predicted dependence of $(dW/dV)^*_{min}$ on a/W (Fig. 10).

Yet another significant contribution of the present investigation lies in the independence of $(dW/dV)^*_p$ from a/W. It is suggested that the parameter $(dW/dV)^*_p$ signifies the global instability in ductile materials and it is a material characteristic.

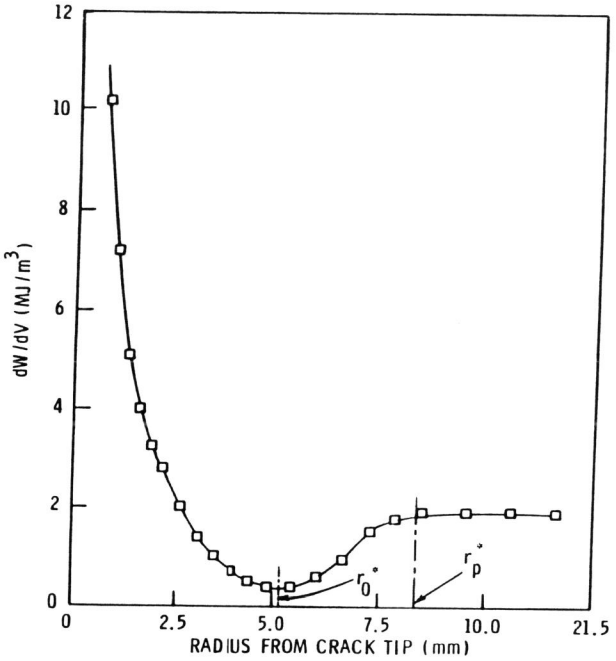

Fig. 6. Unique shape of the local strain energy density versus radial distance (nodes at 0 degree from the crack tip) curve for a crack length of 39.04 mm at a unique load of 22.15 kN (termed the critical load for a crack, 39.04 mm in length).

CONCLUSIONS

Local (nodal) strain energy density results have been computed by two-dimensional non-linear finite element analysis of cracked A-517 steel compact tension specimens over a wide range of crack length-to-width ratio (0.25 to 0.88). The premise behind the numerical investigation is our hypothesis that the local strain energy density should have a unique "signature" associated with the crack growth in a cracked structure irrespective of how the structure is externally loaded. Our investigation reveals that indeed the strain energy density exhibits a unique "signature" in that in the expected crack propagation direction in the compact tension specimens, i.e., 0 degree, the local strain energy density first decreases with increasing distance from crack tip but then at a critical distance it increases and subsequently at a critical load it becomes constant. Based on this unique signature, we have numerically established the following three parameters: (a) a material characteristic global instability energy parameter $(dW/dV)^*_p$ equal to 1.93 MJ/m^3, (b) a crack length dependent local instability energy parameter $(dW/dV)^*_{min}$ equal to about 0.36 MJ/m^3, and (c) a material characteristic non-dimensional parameter, P_{cr}/P_f equal to 0.83, the parameter being the ratio of a critical load which satisfies the

necessary and sufficient conditions for the initiation of crack growth to the predicted fracture load.

ACKNOWLEDGMENT

This investigation was supported by the U.S. Naval Sea Systems Command.

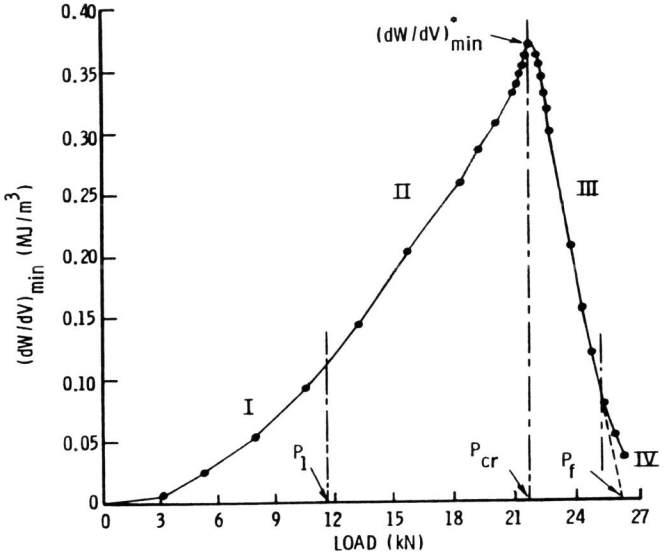

Fig. 7. Plot showing the dependence of minimum strain energy density (as observed in Fig. 5, for example) on load for a crack length of 39.04 mm. $(dW/dV)^*_{min}$ represents the peak value of the minimum strain energy density data and it corresponds to the critical load (P_{cr}) of 22.15 kN.

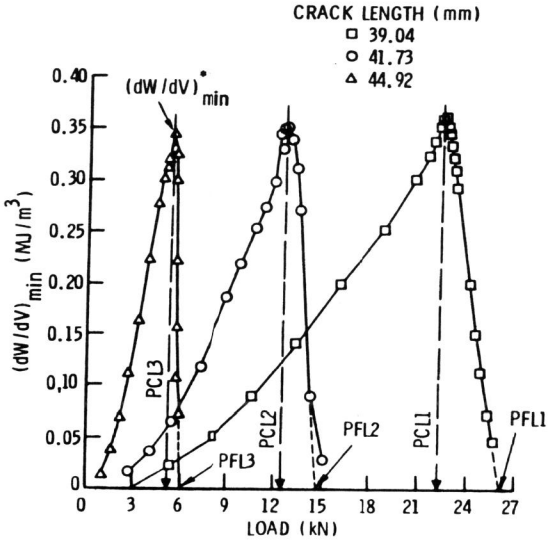

Fig. 8. Comparison of $(dW/dV)_{min}$ versus load plots (as observed in Fig. 7) for three cracks of different lengths. There are three peaks corresponding to the three critical loads (PCL1,PCL2,PCL3; 1,2,3 referring to crack length of 39.04 mm, 41.73 mm and 44.92 mm, respectively). PCL and PFL stand for predicted critical load and predicted fracture load, respectively.

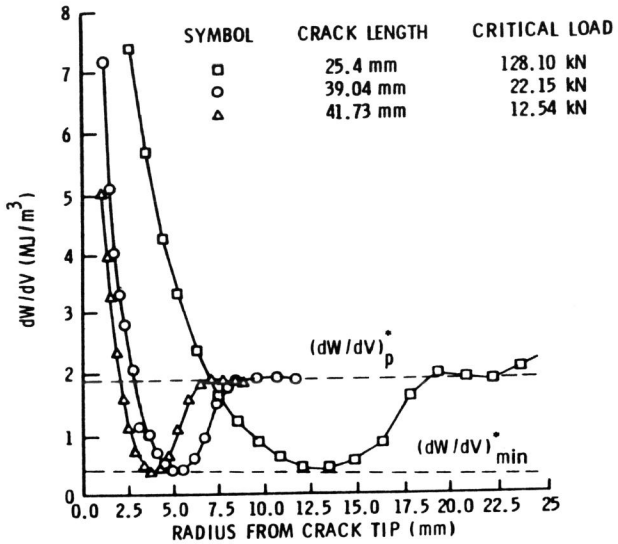

Fig. 9. Comparison of dW/dV versus radial distance plots (as observed in Fig. 6) for three cracks of different length at their predicted critical loads. All the three plots exhibit plateau at a unique value of dW/dV; this constant energy value is designated as $(dW/dV)_p^*$ where the subscript p denotes plateau and the superscript * signifies the critical loads.

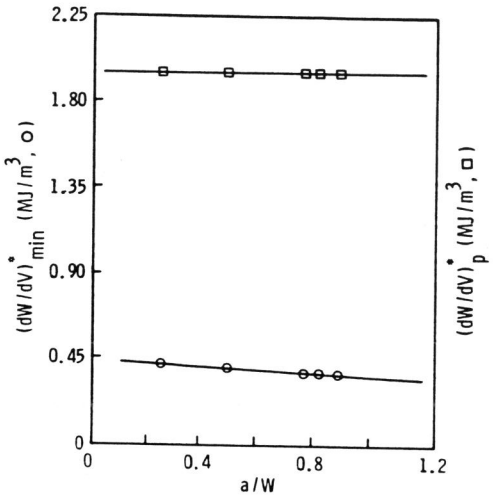

Fig. 10. Plots showing the independence of the critical global instability energy parameter $(dW/dV)^*_p$ and the near-independence of the critical local instability energy parameter $(dW/dV)^*_{min}$ from the crack length-to-width ratio.

REFERENCES

Bathe, K. J. (1982). Finite Element Procedures in Engineering Analysis. Prentice-Hall, New Jersey.

Cook, R. D. (1981). Concept and Applications of Finite Element Analysis (2nd edition). John Wiley & Sons, New York.

de Koning, A. U. (1977). A contribution to the analysis of quasi-static crack. In: Fracture 1977: Advances in Research on the Strength and Fracture of Materials (ICF4) (D. M. R. Taplin, ed.), Vol. 3, pp. 25-31. Pergamon Press, New York.

Gillemot, L. F. (1976). Criterion of crack initiation and spreading. Engineering Fracture Mechanics, 8, 239-253.

Hilton, P. D. and L. N. Gifford (1983). Elastic-plastic finite element analysis of two-dimensional crack problems. In: Elastic-Plastic Fracture (C. F. Shih and J. P. Gudas, eds.), ASTM STP 803, pp. I256-I273. ASTM, Philadelphia.

Hilton, P. D. and G. C. Sih (1973). Application of the finite element method to the calculation of stress intensity factors. In: Mechanics of Fracture: Methods of Analysis and Solutions of Crack Problems (G. C. Sih, ed.), Vol. 1, pp. 426-483. Noordhoff, Leyden.

Hucek, H. J. (1981). Structural Alloys Handbook. Battelle's Columbus Laboratories, Columbus.

Lee, J. D. and H. Liebowitz (1977). The nonlinear and biaxial effects on energy release rate, J-integral and stress intensity factor. Engineering Fracture Mechanics, 9, 765-779.

Owen, D. R. J. and E. Hinton (1980). Finite Element in Plasticity: Theory and Practice. Pineridge Press, Syracuse.

Sih, G. C. (1974). Elastic-plastic fracture mechanics. In: Prospects of Fracture Mechanics (G. D. Sih et al., eds), pp. 613-621. Noordhoff, Leyden.

Sih, G. C. (1977). Mechanics of ductile fracture. In: Fracture Mechanics and Technology (G. C. Sih and C. L. Chow, eds.), Vol. 2, pp. 767-784. Noordhoff, Leyden.

Sih, G. C. and R. J. Hartranft (1980). The concept of fracture mechanics applied to the progressive failure of structural members. Computers and Structures, 12, 813-818.

Sih, G. C. and E. Madenci (1983). Fracture initiaion under gross yielding: strain energy density criterion. Enginering Fracture Mechanics, 18, 667-677.

Twickler, R., M. Twickler and W. Dahl (1983). Two- and three-dimensional elastic-plastic stress analysis for a double edge notched tension specimen. Engineering Fracture Mechanics, 24, 553-565.

Zienkiewicz, O. C. (1983). The Finite Element Method (3rd edition). McGraw-Hill, New York.